THE JOURNAL OF BIOLOGICAL CHEMISTRY

Vol. 260, No. 24, Issue of October 25, pp. 13294–13303, 1985
Printed in U.S.A.

The Minimal Structure Containing the Band 3 Anion Transport Site

A ^{35}Cl NMR STUDY*

(Received for publication, March 22, 1985)

Joseph J. Falke‡, Katherine J. Kanes, and Sunney I. Chan§

From the Arthur Amos Noyes Laboratory of Chemical Physics, California Institute of Technology, Pasadena, California 91125

^{35}Cl NMR, which enables observation of chloride binding to the anion transport site on band 3, is used in the present study to determine the minimal structure containing the intact transport site. Removal of cytoskeletal and other nonintegral membrane proteins, or removal of the 40-kDa cytoskeletal domain of band 3, each leave the transport site intact. Similarly, cleavage of the 52-kDa transport domain into 17- and 35-kDa fragments by chymotrypsin leaves the transport site intact. Extensive proteolysis by papain reduces the integral red cell membrane proteins to their transmembrane segments. Papain treatment removes approximately 60% of the extramembrane portion of the transport domain and produces small fragments primarily in the range 3–7 kDa, with 5 kDa being most predominant. Papain treatment damages, but does not destroy, chloride binding to the transport site; thus, the minimal structure containing the transport site is composed solely of transmembrane segments. In short, the results are completely consistent with a picture in which 1) the transport site is buried in the membrane where it is protected from proteolysis; 2) the transmembrane segments that surround the transport site are held together by strong attractive forces within the bilayer; and 3) the transport site is accessed by solution chloride via an anion channel leading from the transport site to the solution.

The band 3 protein of red cell membranes is a 95-kDa transmembrane protein composed of a single polypeptide chain. The protein exists as a dimer and tetramer in the membrane (reviewed in Ref. 1, but each monomer appears to act as an independent unit in both the anion transport and cytoskeletal functions of band 3 (1–3). The anion transport reaction catalyzed by band 3 is the one-for-one exchange of chloride and bicarbonate: this reaction is central to the respiration of CO_2. As a result, band 3 is the most heavily used ion transport protein in typical vertebrate animals (4). Band 3 also serves as the attachment point on the membrane for the red cell cytoskeleton (5, 6); however, the distinct transport and cytoskeletal functions are associated with different structural domains of the monomer. Proteolysis with trypsin separates these domains and produces both 1) a 52-kDa membrane-bound transport domain that can still catalyze anion exchange (7) and 2) a 40-kDa water-soluble cytoplasmic domain that still binds the cytoskeletal protein ankyrin (8).

The present study focuses on the transport domain. The structure of this domain could be quite complicated since the transport domain contains at least seven different transmembrane segments. Proteolytic studies have played an important role in the development of the current picture of the transmembrane folding pattern of band 3: proteolytic cleavage sites relevant to the present work are indicated in Fig. 1. Intracellular trypsin (9, 10) or chymotrypsin (9, 11) removes the cytoplasmic domain from the transport domain, while extracellular chymotrypsin (9, 11, 12) or papain (13) produces cleavages within the transport domain (Fig. 1). Recently, about five of the transmembrane segments have been generated by proteolysis; extensive cleavage of both sides of the membrane with the nonspecific protease pepsin produced a mixture of small fragments, each large enough to span the membrane (14).

The transport domain contains a single transport site that is alternately exposed to opposite sides of the membrane during the transport cycle (1, 15). This transport site is known to contain one or more essential arginine residues (16–18), but the location of these residues within the primary structure of the transport domain has not yet been determined. Chemical cross-linking and labeling studies indicate that multiple regions of the transport domain's primary structure are in close proximity to the transport site. In particular, the fragments that are generated by extracellular chymotrypsin or papain can be covalently cross-linked by 4,4′-diisothiocyanodihydrostilbene-2,2′-disulfonate (H_2DIDS),[1] an anionic inhibitor that binds reversibly to the transport site before reacting covalently at two lysine residues in the vicinity of the transport site (19, 20). Similarly, 4,4′-diisothiocyanostilbene-2-2′-disulfonate (DIDS) (21), 4-isothiocyanobenzenesulfonate (22), 3,5-diiodo-4-isothiocyanobenzenesulfonate (23), and dinitrofluorobenzene (24) all irreversibly inhibit transport by covalently attaching to the 17-kDa chymotryptic fragment (Fig. 1), while phenylglyoxal (PG) (25), pyridoxal-5-phosphate (26), and reductive methylation of lysine all irreversibly inhibit transport by covalently attaching to the 35-kDa chymotryptic fragment (Fig. 1). In addition, inhibitors that attach to the 17-kDa fragment (4-isothiocyanobenzene-

* This work was supported by National Institute of General Medical Sciences Grant GM-22432 (to S. I. C.) and by a National Science Foundation predoctoral fellowship (to J. J. F.). This is contribution 7096 from the Arthur Amos Noyes Laboratory of Chemical Physics. The costs of publication of this article were defrayed in part by the payment of page charges. This article must therefore be hereby marked "*advertisement*" in accordance with 18 U.S.C. Section 1734 solely to indicate this fact.

‡ Present address: Department of Biochemistry, University of California, Berkeley, CA 94720.

§ To whom reprint requests should be addressed.

[1] The abbreviations used are: H_2DIDS, 4,4′-diisothiocyano-2-2′-dihydrostilbene disulfonate; DIDS, 4,4′-diisothiocyanostilbene-2,2′-disulfonate; DNDS, 4,4′-dinitrostilbene-2,2′-disulfonate; SDS-PAGE, sodium dodecyl sulfate-polyacrylamide gel electrophoresis; PBS, 150 mM NaCl, 10 mM NaH_2PO_4, pH 7.4, with NaOH; 5P8, 5 mM NaH_2PO_4, pH 8.0, with NaOH; BSA, bovine serum albumin; PMSF, phenylmethylsulfonyl fluoride; BME, β-mercaptoethanol; PG, phenylglyoxal; TEMED, *N,N,N′,N′*-tetramethylethylenediamine.

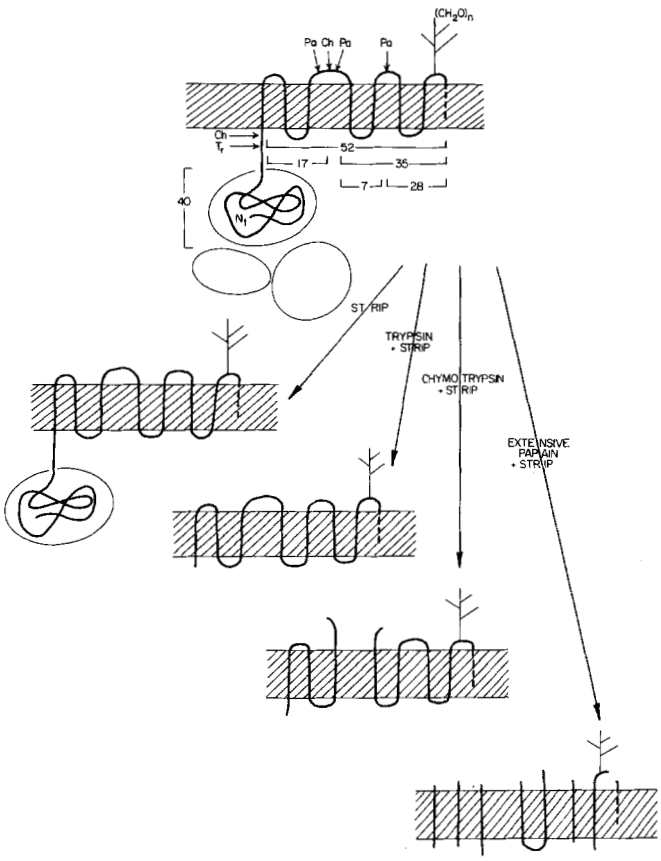

FIG. 1. **Summary of the stripping and proteolytic treatments employed.** Shown is the current model for the transmembrane structure of the transport domain of band 3. Also shown is the cytoplasmic domain of band 3 (*circled*), as well as cytoplasmic proteins nonintegrally associated with the membrane. The proteolytic cleavage sites indicated by the *arrows* are for trypsin (*Tr*), chymotrypsin (*Ch*), and papain (*Pa*).

sulfonate and dinitrofluorobenzene), as well as inhibitors that attach to the 35-kDa frament (PG, pyridoxal-5-phosphate, and reductive methylation of lysine), each have been shown to overlap the binding site for the stilbenedisulfonates, which are known to occupy the transport site (1, 2). Thus, it is likely that the structure of the transport site has contributions from multiple regions within the primary structure.

The present study investigates the location of the transport site within the transport domain. The strategy of this search is straight-forward: first, a nonessential protein or peptide is removed from the transport domain by stripping away nonintegral proteins from the membrane or by proteolysis of the membrane; then ^{35}Cl NMR is used to ascertain whether the transport site can still bind chloride. The results indicate that the transport site remains fully intact following 1) removal of nonintegral red cell membrane proteins by high pH stripping, 2) removal of the band 3 cytoplasmic domain by trypsin or chymotrypsin, or 3) cleavage of the band 3 transport domain by chymotrypsin. It is also shown that extensive proteolysis on both sides of the membrane with the nonspecific protease papain produces a mixture of small fragments of appropriate size to be transmembrane segments. Chloride binding to the transport site is still observed for these membrane-bound fragments; thus, the transport site is buried within the membrane where it is protected from proteolysis, and the site is composed of residues from one or more of the papain-generated transmembrane segments.

MATERIALS AND METHODS

Reagents—Freshly outdated human blood (packed red cells) was a kind gift of the Los Angeles Chapter of the American Red Cross. Used without further purification were: trypsin and α-chymotrypsin (Worthington); papain (Calbiochem); H_2DIDS (Molecular Probes); phenylglyoxal (Aldrich); SDS (specially pure from BHD Chemicals); acrylamide, bisacrylamide, TEMED, and ammonium persulfate (electrophoresis grade from Bio-Rad); urea (ultra-pure from Schwarz/Mann); and glycine (ammonia-free from Sigma). Electrophoresis calibration proteins were from Pharmacia (low molecular weight calibration kit), Boehringer Mannheim (aprotinin), and Sigma (insulin A).

H_2DIDS Labeling of Red Cells—Where appropriate, intact red cells labeled with H_2DIDS, as well as unlabeled control cells, were prepared from intact red cells. First, red cells were washed 3 times in PBS, with simultaneous removal of the buffy coat (4). Then cells to be labeled and control cells were incubated ±20 μM H_2DIDS in PBS, 37 °C for 1 h, followed by two washes in PBS + 0.2% BSA, and one wash in PBS before undertaking the standard ghost preparation.

Preparation of Ghost Membranes—Leaky isolated red cell membranes, or ghosts, were prepared and stored exactly as previously described (4). Unless otherwise indicated, all further manipulations of membranes were on ice, all subsequent washes of ghost membranes or modified ghost membranes were 20,000 rpm (48,000 × g_{max})/15 min in a Sorvall SS-34 rotor, 0°C, and in all washes the pellet was diluted to <1/10 original concentration.

Phenylglyoxal Labeling of Ghost Membranes—Where appropriate, the pellet from the ghost preparation was diluted to 3/5 original concentration and incubated in 20 mM PG ± 2 mM DNDS in 80 mM boric acid, pH to 8.0 with NaOH, 37°C for 30 min. The ghosts were then washed twice in 5P8 (thus, a total of four washes in 5P8 before proteolysis, see below).

Proteolysis of Ghost Membranes—Unlabeled ghosts, or ghosts labeled with H_2DIDS or phenylglyoxal, were washed twice in 5P8. The resulting pellet was resuspended in >10 volumes of a control solution or a protease-containing solution and incubated as appropriate: trypsin (±30 μg/ml, 40 mM NaCl, 5P8, 0°C for 1 h), chymotrypsin (±100 μg/ml, 5P8, 23°C for 45 min), and papain (±10 mg/ml, 50 mM Na acetate, pH 5.2, with acetic, 4 mM cysteine-HCl, pH 5.2, with NaOH, 37°C for 1 h, with vortexing every 5 min to prevent excessive aggregation of membranes). The protease was then removed by washing once in 5P8 containing the protease inhibitor PMSF (100 μg/ml). The papain-treated membranes sometimes form a dense pellet that is difficult to resuspend to homogeneity by vortexing; in such cases the pellet was resuspended by repeatedly passing the suspension through a Pasteur pipette.

High pH Stripping of Ghost Membranes—Ghosts or modified ghosts prepared as above were stripped of nonintegral proteins or proteolytic fragments by exposure to high pH at low ionic strength. Membranes were washed once in 5P8, once in H_2O, once in 10 mM NaOH, and again in H_2O. The pH was then lowered by immediately performing the high-salt wash.

High-salt Washing of Ghost Membranes—Proteins or proteolytic fragments that adhere to the membrane via salt bridges were eluted from the membrane by high-salt washes. Ghosts or modified ghosts were washed once in 250 mM NH_4Cl, 5P8, pH to 8.0, with NaOH, NH_4OH, then once in 100 mM NH_4Cl, 5P8, pH to 8.0, with NaOH, NH_4OH.

NMR Sample Preparation—The pellet from each of the above preparations was resuspended in 100 mM NH_4Cl, 5P8, pH to 8.0, with NaOH, NH_4OH, to a volume equal to the original volume of ghosts used to make that sample. An exception was made for papain-treated membranes, which were resuspended to ¼ of their original volume to counteract the decrease in the transport site $^{35}Cl^-$ linebroadening caused by papain (see Fig. 7). The resulting suspensions were sonicated to disrupt sealed vesicles, crushed ghosts, or aggregates of ghosts (15); then the membranes were aliquoted and NMR samples were prepared exactly as previously described (4). In order to determine the $^{35}Cl^-$ linebroadening due to band 3 transport sites, the same volume of H_2O or DNDS stock solution was added to identical samples. The transport site linebroadening is given by the linebroadening inhibited by 1 mM DNDS and is also termed the DNDS-sensitive linebroadening (4). All samples were prepared from red cells the same day that they were used for ^{35}Cl NMR.

^{35}Cl NMR Spectroscopy—Spectra were obtained at 3°C on a JEOL EX-90Q spectrometer (^{35}Cl:8.8 MHz). The standard spectral param-

eters were the same as those previously described (4), except that 200 dummy scans were performed immediately before the acquisition scans in order to ensure equilibration of sample temperature to that of the probe; this equilibration minimizes the experimental error in linebroadening determinations.

NMR Sample Analysis—$^{35}Cl^-$ linebroadenings from different samples were corrected for differences in band 3 concentration by normalizing to the same cholesterol concentration, since the ratio of band 3/cholesterol must be the same for membranes made from the same batch of red cells. To determine cholesterol, the membrane lipids were first extracted by adding 1 ml of sample (0.2–0.4 mg of cholesterol) to 19 ml of $CHCl_3$:MeOH (2:1) and vortexing until mixed. The protein precipitate was removed by suction filtration, and 2 ml of H_2O was added to the filtrate, with vortexing to ensure equilibration of soluble components between the newly forming organic and aqueous phases. A particular volume (typically 12 ml) of the organic phase was removed using a separatory funnel and placed in a hot water bath to boil off the solvent. Then the lipids were dissolved in 5 ml of $CHCl_3$ and the Liebermann-Buchard reaction was performed to determine cholesterol as previously described (27).

Preparation of Electrophoresis Samples—Membranes or modified membranes prepared as above were washed in 5P8 and kept on ice. One volume of membranes was then added to 1 volume of Laemmli sample buffer (30% glycerol, 80 mM dithiothreitol, 4% SDS, 130 mM Tris base, 5 mg/100 ml bromphenol blue), vortexed, and incubated at 100°C for 3 min. Where appropriate, membrane components were first separated into organophyllic and organophobic fractions by extraction with $CHCl_3$:MeOH (2:1). One volume of membranes (protein ≥1 mg/ml) was added to 20 volumes of $CHCl_3$:MeOH (2:1) in a Corex (Sorvall) centrifuge tube, with vortexing. The organophobic components that precipitate were pelleted by spinning at 10,000 rpm for 30 min in a Sorvall SS-34 rotor. Being careful to save the pellet, the supernatant containing the organophilic components was poured into a clean tube and the solvent was boiled off in a hot H_2O bath. The resulting organophobic and organophilic fractions were resolubilized in 2 volumes of 2% SDS, 1% BME, 8 M urea by vortexing and washing of the sides of the tubes with a Pasteur pipette; the resolubilization was aided by sonication for >30 min in a bath sonicator. The solubilized samples were then diluted with Laemmli sample buffer and heated as above. Membranes to be used for gel samples were stored <1 day at 4°C or >1 day at −80°C. Following addition of Laemmli sample buffer, the samples were stored at room temperature for no more than 2 days.

Electrophoresis—Two gel systems were employed for high- and low-molecular weight ranges. Both systems used the discontinuous buffer system of Laemmli (28). For the high molecular weight gel, the stacking gel contained 4% (w/v) acrylamide and 0.053% bisacrylamide, and the separatory gel contained 10% acrylamide and 0.13% bisacrylamide. High molecular weight gels were stained with Coomassie Blue as previously described (29). For the low molecular weight gel, the stacking gel contained 9.6% acrylamide and 0.048% bisacrylamide, and the separatory gel contained 16% acrylamide, 0.5% bisacrylamide, 21.6% urea, and 13.3% glycerol (v/v). The low molecular weight stacking and separatory solutions were filtered and copolymerized (30). Low molecular weight gels were silver-stained as previously described (31), except that gels were first fixed in 10% trichloroacetic acid, 40% MeOH for >4 h, and all solutions before the staining solution and after the reducing solution contained 40% MeOH to prevent gel swelling. Photographs and negatives were obtained using a Polaroid land camera and Type 55 Polaroid film. Molecular weights were determined from a standard plot of migration (relative to the leading edge of the stack) *versus* $\log_{10} M_r$ for the following standard proteins; phosphorylase *b* (94,000), BSA (67,000), ovalbumin (43,000), carbonic anhydrase (30,000), soybean trypsin inhibitor (20,100), lactalbumin (14,400), aprotinin (6,500), and insulin A (2,300).

RESULTS

Observation of Band 3 Transport Sites by ^{35}Cl NMR—The minimal structure containing the intact band 3 transport site can be identified only if it is possible to monitor the intactness of the site. We have recently shown that ^{35}Cl NMR provides a sensitive assay for chloride binding to band 3 transport sites on both sides of the red cell membrane (4, 15). The physical basis of this technique is the large ^{35}Cl NMR spectral width of chloride in a macromolecular binding site; the bound chloride spectral width is typically at least $\geq 10^4$ times larger than the linewidth of chloride in solution. As a result, when solution chloride samples a binding site sufficiently rapidly, the site can cause measurable broadening of the solution chloride linewidth. This increase in linewidth, or linebroadening, contains information on the structure and motions of the site and on the rate of chloride migration between the site and solution (32, 33). The linebroadening due to a given site is directly proportional to the fraction of the total chloride which is bound to the site, and the linebroadening due to different sites are additive. As a result, the $^{35}Cl^-$ linebroadening due to a heterogeneous population of chloride binding sites is given by Equation 1 (4)

$$\delta = \sum_j \alpha_j \frac{[Cl^-]_{B_j}}{[Cl^-]} = \sum_j \frac{\alpha_j [E_j]_T}{K_{D_j}} \frac{[Cl^-]^{-1}}{[Cl^-]^{-1} + K_{D_j}^{-1}} \quad (1)$$

where the sum is over the different types of sites E_j. The quantities $[Cl^-]_{B_j}$ and $[Cl^-]$ are the concentrations of chloride bound to the jth type of site and the total chloride concentration, respectively. α_j is a constant characteristic of the jth type of site, K_{D_j} is the chloride dissociation constant of the jth type of site, and $[E_j]_T$ is the total concentration of the jth type of site. Equation 1 assumes that the bound chloride returns to solution before binding to another site and that the bound chloride concentration is negligible relative to the total chloride concentration. In the red cell membrane system, multiple types of chloride binding sites are observed (4). The additive contribution of the transport site to the total red cell membrane linebroadening can be determined using DNDS, an anionic reversible inhibitor of the transport site, to identify the transport site linebroadening. For a homogeneous class of sites, the linebroadening is shown in Equation 2 (4).

$$\delta_j = \frac{\alpha_j [E_j]_T}{K_{D_j}} \frac{[Cl^-]^{-1}}{[Cl^-]^{-1} + K_{D_j}^{-1}} \quad (2)$$

This equation indicates that a high-affinity site ($K_{D_j} \lesssim [Cl^-]$) gives rise to a square hyperbola on a plot of $^{35}Cl^-$ linebroadening *versus* $[Cl^-]^{-1}$, while a low-affinity site ($K_{D_j} \gg [Cl^-]$) gives rise to a straight line of zero slope. Thus, $^{35}Cl^-$ linebroadening *versus* $[Cl^-]^{-1}$ data can be used to study the effects of removal of nonintegral proteins and of proteolysis on the integrity of the transport site.

The Effect of Nonintegral Proteins on the Transport Site—Isolated red cell membranes or ghosts possess a variety of protein constituents. It is generally assumed that the chloride transport unit is localized completely within band 3, but it is possible that another unidentified protein(s) could be required for the structural integrity of the transport unit. Several distinct classes of proteins exist in the ghost membrane system including (34); 1) transmembrane integral proteins such as band 3, glycophorin, the glucose transporter, and the Na,K-ATPase; 2) nonintegral cytoskeletal proteins including spectrin, actin, bands 4.1 and 4.2, and ankyrin; and 3) nonintegral cytoplasmic proteins that bind to band 3 such as hemoglobin and glyceraldehyde-3-phosphate dehydrogenase. The nonintegral proteins can easily be removed from the ghost membrane; thus, it is possible to test for interactions between these proteins and the transport site.

The two methods used here for the removal of nonintegral proteins are high-salt extraction and high-pH stripping. High-salt extraction disrupts ionic interactions and releases at least one protein, glyceraldehyde-3-phosphate dehydrogenase, from the membrane. High-pH stripping at low ionic strength removes virtually all of the nonintegral proteins; the mechanism of this stripping involves generation of a negative surface

charge on the proteins and the membrane, which at low ionic strength repels the nonintegral proteins from the membrane (35). The effects of high-salt extraction and high-pH stripping on the protein composition of ghost membranes are shown in Fig. 2. SDS-polyacrylamide gel electrophoresis indicates that a large number of proteins exist in untreated ghost membranes and a high-salt wash removes glyceraldehyde-3-phosphate dehydrogenase, while high-pH stripping followed by a high-salt wash removes most of the bands and leaves band 3 as the major protein constituent (70% of the remaining proteins (1)). In each case, band 3 migrates as a broad band due to heterogeneous glycosylation of the membrane-bound transport domain (36).

The effect of nonintegral protein removal on the $^{35}Cl^-$ linebroadening due to the band 3 transport site is shown in Fig. 3. Transport site linebroadening *versus* $[Cl^-]^{-1}$ data are shown for three types of sonicated ghost membranes: 1) control membranes (ghosts), 2) membranes extracted with high salt (washed ghosts), and 3) membranes stripped with high pH at low ionic strength then extracted with high salt (stripped ghosts). These membrane samples correspond to the SDS-PAGE *lanes b–d* in Fig. 2, respectively. The data for these three cases are indistinguishable, and the average dissociation constant for chloride binding in the three cases is $K_D = 50 \pm 15$ mM, which is within experimental error of the previously determined $K_D = 80 \pm 20$ mM for chloride binding to band 3 transport sites on leaky ghost membranes (4). Thus, the nonintegral proteins have no measurable effect on the integrity of the transport site.

The Effect of the Cytoskeletal Domain on the Transport Site—The 40-kDa cytoskeletal domain of band 3 lies on the cytoplasmic surface of the membrane, where it binds the cytoskeletal protein ankyrin and other cytoplasmic proteins (34). Proteolysis can be used to quantitatively remove the cytoskeletal domain from the transport domain; thus, the proposal that the transport domain is structurally independent of the cytoskeletal domain can be easily tested. Trypsinization of leaky ghosts followed by stripping yields the 52-kDa transport domain, which migrates as a broad band due to heterogeneous glycosylation. A previously noted characteristic feature of this band is the higher staining intensity at its leading edge (13). In the present experiments the observation of this characteristic band confirms the removal of the cytoskeletal domain by trypsin (Fig. 2, *lane f*).

The effect of removal of the cytoskeletal domain on the $^{35}Cl^-$ linebroadening due to band 3 transport sites is shown in Fig. 3. Transport site linebroadening *versus* $[Cl^-]^{-1}$ data are shown for two types of sonicated ghost membranes: 1) stripped ghosts and 2) stripped trypsinized ghosts. These membranes samples correspond to the SDS-PAGE *lanes e* and *f* in Fig. 2, respectively. The data indicate that removal of the cytoplasmic fragment does not inhibit the transport site linebroadening; instead, a slight increase (23%) in the transport site linebroadening is observed. It is not possible to specify the mechanism of this linebroadening increase; it could involve a small change in the structure of the band 3 transport domain, including a possible redistribution of the transport site between the inward- and outward-facing con-

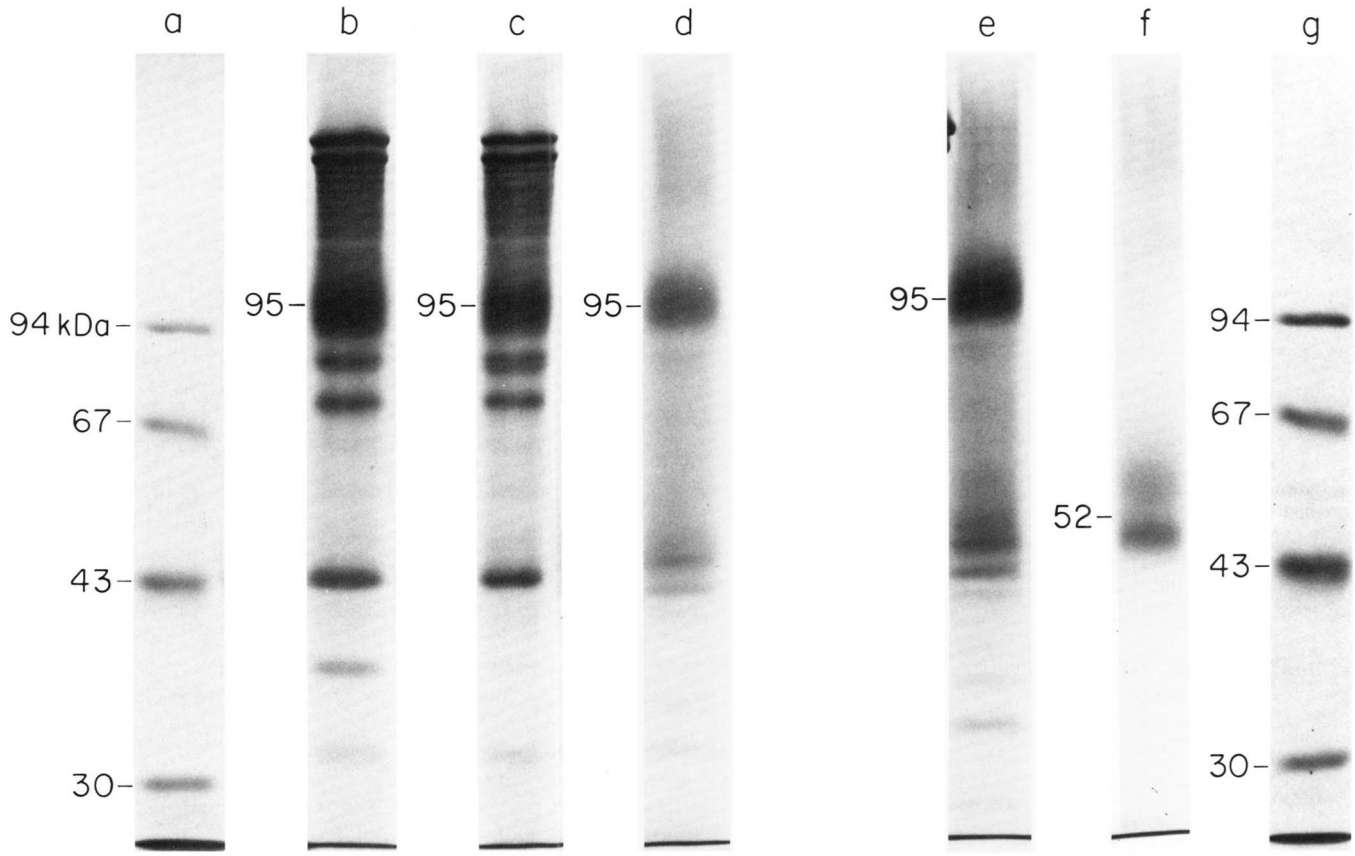

FIG. 2. **Removal of nonintegral red cell membrane proteins and removal of the band 3 cytoskeletal domain.** Shown are the SDS-polyacrylamide gel electrophoresis patterns of *lanes a* and *g*, molecular weight markers; *lane b*, ghosts; *lane c*, ghosts washed in high salt; *lanes d* and *e*, ghosts stripped with high pH at low ionic strength, then washed in high salt; and *lane f*, trypsinized ghosts stripped with high pH at low ionic strength, then washed in high salt. Lanes *a–d* and *e* and *f* were run on two different gels, respectively. The high-molecular weight gel system was as described in text.

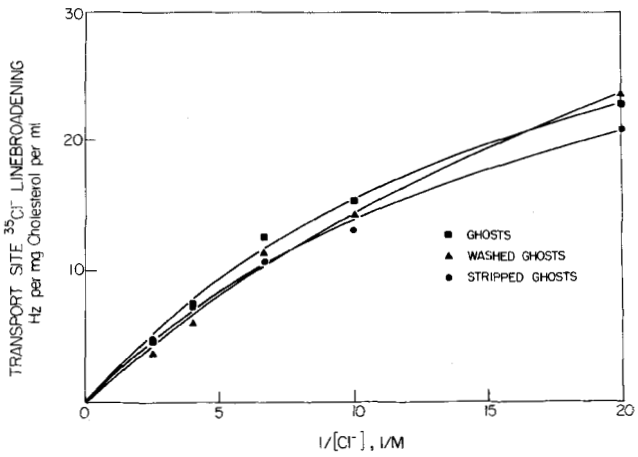

FIG. 3. **The effect on band 3 transport sites of removal of nonintegral proteins.** Shown is the $^{35}Cl^-$ linebroadening due to band 3 transport sites on sonicated ghost membranes (*ghosts*), ghost membranes washed in high salt then sonicated (*washed ghosts*), and ghost membranes stripped with high pH at low ionic strength, then washed in high salt and sonicated (*stripped ghosts*). Samples contained x mM NH_4Cl, ionic strength to $(400 - x)$ mM with Na citrate, 5 mM NaH_2PO_4, 20% D_2O, pH to 8, with NaOH and NH_4OH. ^{35}Cl NMR spectra were obtained at 8.8 MHz and 3°C. The nonlinear least-squares best-fit curves ($y = Ax/(1 + xK_D)$, *solid lines*) yielded an average $K_D = 50 \pm 15$ mM for chloride binding in the three cases.

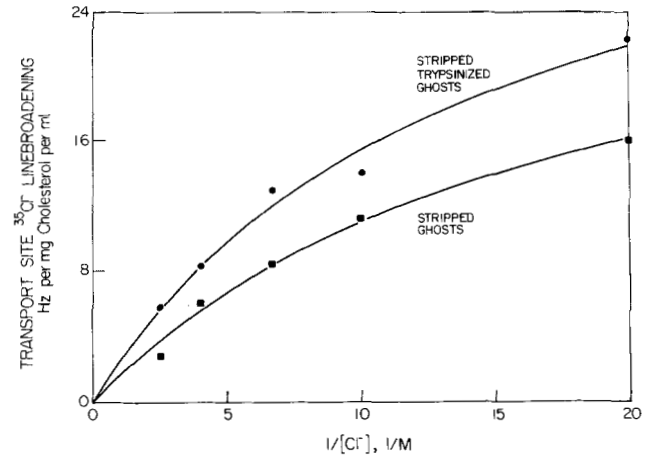

FIG. 4. **The effect on band 3 transport sites of removal of nonintegral protein.** Shown is the $^{35}Cl^-$ linebroadening due to band 3 transport sites on ghost membranes (*stripped ghosts*) and trypsinized ghost membranes (*stripped trypsinized ghosts*). Both types of membranes were stripped with high pH at low ionic strength then washed in high salt and sonicated. Samples and ^{35}Cl NMR spectra were as in Fig. 3. The nonlinear least-squares best-fit curves ($y = Ax/(1 + xK_D)$, *solid lines*) yielded $K_D = 60 \pm 10$ mM and $K_D = 70 \pm 10$ mM for chloride binding to transport sites on stripped ghosts and stripped trypsinized ghosts, respectively.

formations, or an increase in the rate of chloride migration between the transport site and solution (4, 33). The structure of the transport site is not significantly affected, however, since the chloride dissociation constant for the site is essentially the same with ($K_D = 60 \pm 10$ mM) or without ($K_D = 70 \pm 10$ mM) the cytoskeletal domain (Fig. 4). These results are completely consistent with previous anion transport results, indicating that transport remains 50% (37) to 100% (7) intact following removal of the cytoskeletal domain with trypsin. Thus, the cytoskeletal domain is not essential for the structure of the transport site.

The Effect of Proteolytic Cleavage within the Transport Domain on the Transport Site—Treatment of leaky ghosts with chymotrypsin releases the cytoskeletal domain from the transport domain and also produces a second cleavage within the transport domain at the extracellular surface (Fig. 1). Since it has just been shown that removal of the cytoskeletal domain leaves the transport site intact, chymotrypsin can be used to examine the effect of cleavage within the transport domain on the transport site.

Chymotryptic digestion of leaky ghosts produces 35- and 17-kDa fragments of the transport domain (Fig. 1). The 35-kDa fragment gives rise to a broad band that is generally not observed on SDS-PAGE gels due to heterogeneous glycosylation (38, 39). In contrast, the 17-kDa fragment gives rise to a sharp band. In the present experiments observation of the characteristic band due to the 17-kDa fragment confirms the removal of the cytoskeletal domain and the internal cleavage of the transport domain (Fig. 5, *lane b*).

The effect of the two chymotryptic cleavages on the $^{35}Cl^-$ linebroadening due to band 3 transport sites is shown in Fig. 6. Transport site linebroadening *versus* $[Cl^-]^{-1}$ data are shown for two types of sonicated ghost membranes: 1) stripped ghosts and 2) stripped chymotrypsinized ghosts, where the stripped chymotrypsinized membranes correspond to SDS-PAGE *lane b* in Fig. 5. The data indicate that removal of the cytoplasmic domain and cleavage of the transport domain into 17- and 35-kDa fragments causes a slight increase (~30%) in the transport site linebroadening. Since the same result is observed for the removal of the cytoplasmic domain alone (Fig. 4), it can be concluded that the chymotryptic cleavage within the transport domain has no additional effect on the transport site linebroadening. The structure of the transport site is not significantly changed by the chymotryptic cleavages since the chloride dissociation constant of the control membranes ($K_D = 80 \pm 10$ mM) is essentially the same as that of the chymotrypsinized membranes ($K_D = 70 \pm 2$ mM) (Fig. 6). These results are completely consistent with transport studies conducted on a similar system; extracellular chymotrypsin produces the same 35-kDa fragment as well as 60-kDa fragment containing the cytoskeletal domain. Subsequent removal of the cytoskeletal domain with trypsin yields membranes containing 17- and 35-kDa fragments of the transport domain (Fig. 1); in this case, transport remains 80% intact (7). Thus, the 17- and 35-kDa fragments of the transport domain retain the transport site. By analogy with the stable association of the 60- and 35-kDa products of external chymotrypsin, the 17- and 35-kDa chymotryptic fragments may remain associated in the membrane. Therefore, the transport site could be composed of residues from both fragments.

The Peptides Produced by Extensive Papain Digestion of Leaky Ghosts—Recently it has been shown that extensive digestion of leaky ghost membranes with the nonspecific protease pepsin produces a mixture of fragments of the appropriate size to be transmembrane segments (the observed fragments are approximately 4 kDa (14)). Papain is also well-suited for generating transmembrane segments; this protein is one of the most nonspecific and active proteases known, the optimal pH of papain (pH 6.5) is considerably higher than that of pepsin (pH 3.0), and extensive extracellular papain treatment of intact red cells slows transport 75% (40) or 90% (41) but appears to leave the outward-facing transport site intact (41). Thus, papain is used in the present study to generate small transmembrane fragments from band 3 in a search for the minimal structure containing the band 3 transport site.

Extensive papain treatment (10 mg/ml of papain, pH 6.5, 37°C for 1 h) followed by stripping yields the proteolytic fragments indicated in *lane c* of Fig. 5. Nearly all (>90%) of

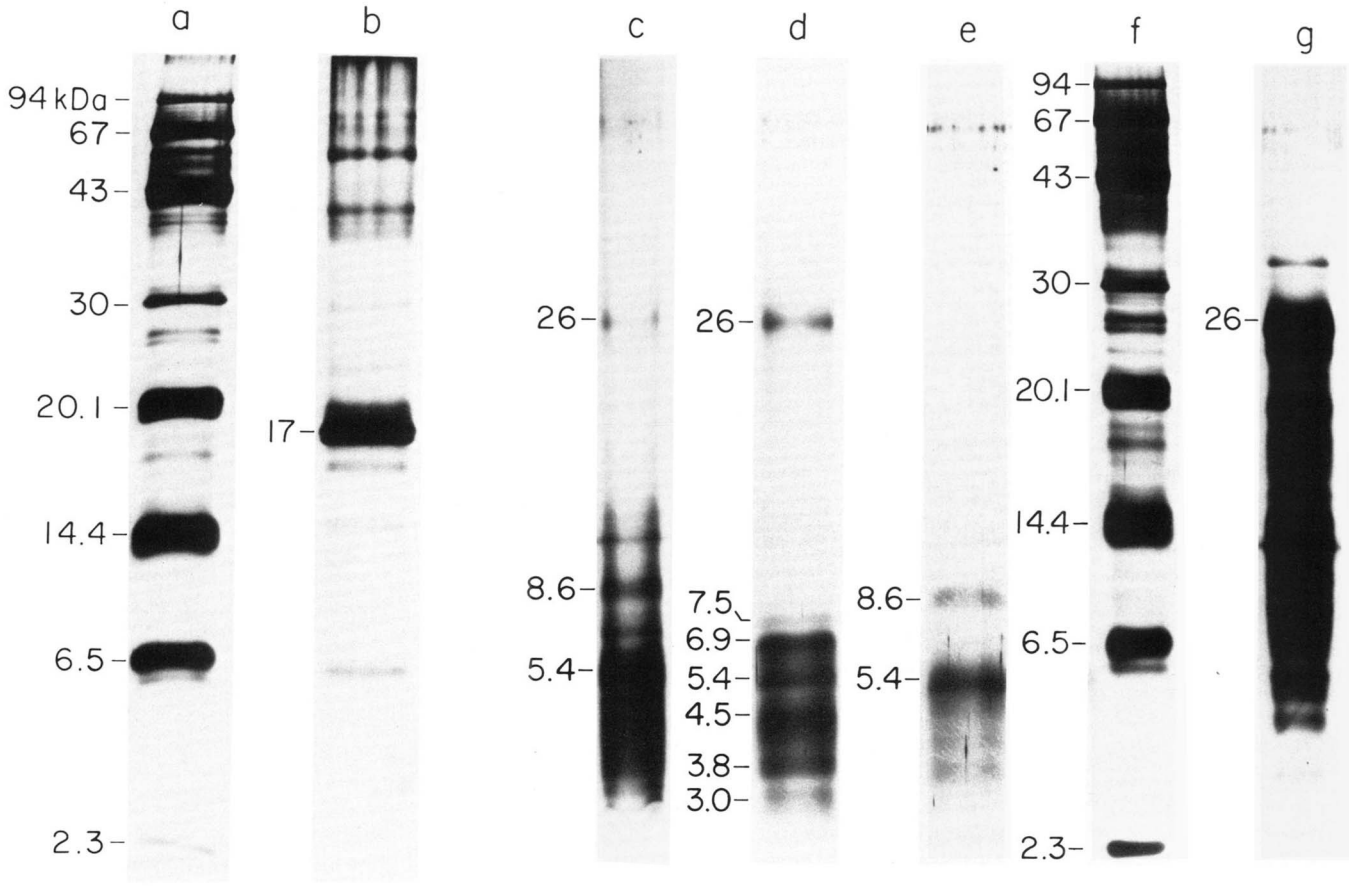

FIG. 5. **Cleavage of the band 3 transport domain by chymotrypsin and papain.** Shown are the SDS-polyacrylamide gel electrophoresis patterns of *lanes a* and *f*, molecular weight markers; *lane b*, chymotrypsinized ghost membranes; *lane c*, papain-treated ghost membranes; *lane d*, the precipitate from $CHCl_3$:MeOH (2:1) extraction of papain-treated ghost membranes; *lane e*, the supernatant from same extraction of papain-treated ghost membranes; and *lane f*, papain with its self-proteolysis fragments (10 mg/ml of papain, 37°C for 1 h). All membrane samples were stripped with high pH at low ionic strength and washed in high salt. *Lanes a* and *b*, and *c* and *g*, were run on two different gels, respectively. The low molecular weight gel system was as described in text.

the resulting fragments are smaller than the molecular weight standard aprotinin (6.5 kDa) and larger than the molecular weight standard insulin A (2.3 kDa). Thus, the range in apparent size of these fragments is approximately 3–7 kDa (Fig. 5, *lane c*). The fragments are clearly a heterogeneous mixture, and the significant background staining observed below 5 kDa suggests that nonspecific proteolysis has resulted in heterogeneous copies of one or more fragments (Fig. 5, *lane c*). However, superimposed on this background are fragments that give rise to discrete bands. These discrete fragments become more visible after the membrane samples are extracted with $CHCl_3$:MeOH (2:1) to separate the peptides into two fractions that are soluble (organophilic) or insoluble (organophobic) in the organic solvent, respectively (Fig. 5, *lanes d* and *e*). At least two organophilic fragments (5.4 and 8.6 kDa) and seven organophobic fragments (3.0, 3.8, 4.5, 5.4, 6.9, 7.5, and 26 kDa) are observed as discrete bands (Fig. 5, *lanes d* and *e*). Excluding the 26-kDa fragment, which may be residual papain (see below), each of the other fragments is long enough to span the membrane only once or twice, assuming that a single α-helical membrane-spanning segment must be at least 3 kDa (see "Discussion"). The relative intensities of the discrete bands in both the organophilic and organophobic fractions should not be used for quantitation since, during the preparation of both fractions, the fragments are precipitated and do not redissolve completely, so that differential resolubilization may occur.

Only two of the discrete fragments can be tentatively identified at the present time. The 26-kDa organophobic fragment appears to be residual papain, which co-migrates with this fragment despite the fact that papain is known to be a 21-kDa polypeptide (42). No other discrete fragments co-migrate with papain or the products of its self-proteolysis (Fig. 5, *lane g*). Moreover, the discrete fragments are too abundant to be products of papain self-proteolysis, since papain is nearly completely removed by membrane washing (compare the 26-kDa fragment in Fig. 5, *lanes c* and *g*). The 8.6-kDa organophilic fragment may be identical to a fragment produced by extracellular cleavage of band 3 by papain; the latter is known to be a 7.5-kDa polypeptide that is soluble in $CHCl_3$:MeOH (2:1) (13). The discrete bands smaller than 8 kDa are all previously undescribed and could be fragments of any of the major integral ghost proteins: band 3 (1×10^6 copies/ghost (1, 2)), glycophorin (5×10^5 copies/ghost (43)), or the glucose transporter (estimated 3×10^5 copies/ghost (44)). Some of the observed fragments may contain two transmembrane segments; thus, the eight or more fragments observed in the range 3–8.6 kDa could include all seven or more of the band 3 transmembrane segments. It should be noted, however, that the single site of glycosylation on band 3 (45) may remain on one of the transmembrane segments. In this event, the broad band due to this heterogeneously glycosylated fragment would not be observed on SDS-PAGE gels.

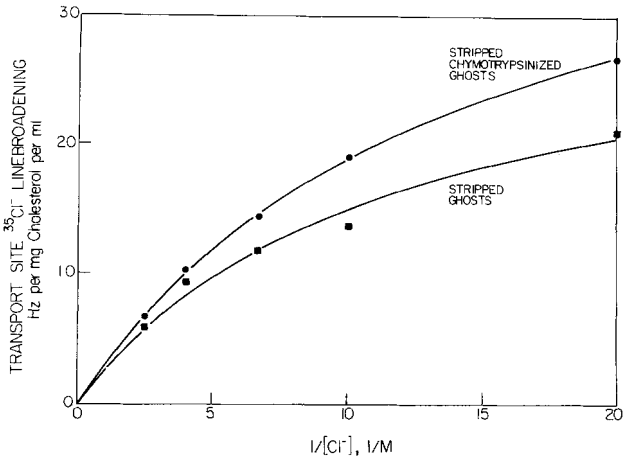

FIG. 6. **The effect on band 3 transport sites of chymotrypsin cleavage within the transport domain.** Shown is the $^{35}Cl^-$ linebroadening due to band 3 transport sites on ghost membranes (*stripped ghosts*) and chymotrypsinized ghost membranes (*stripped chymotrypsinized ghosts*). Both types of membranes were stripped with high pH at low ionic strength, then washed in high salt and sonicated. Samples and ^{35}Cl NMR spectra were as in Fig. 3. The nonlinear least-squares best-fit curves ($y = Ax/(1 + xK_D)$, *solid lines*) yielded $K_D = 80 \pm 10$ mM and $K_D = 70 \pm 2$ mM for chloride binding to the transport sites on stripped ghosts and stripped trypsinized ghosts, respectively.

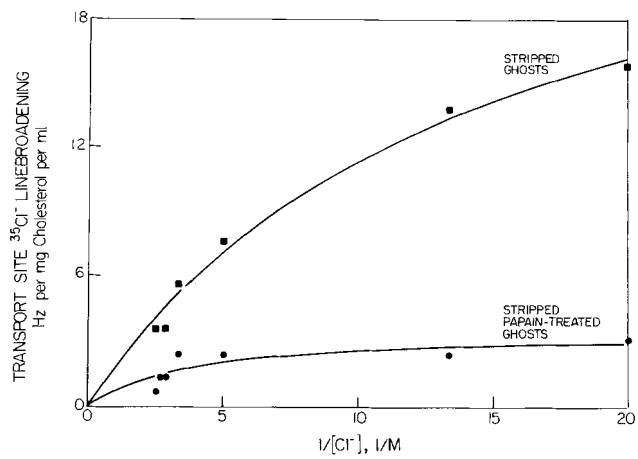

FIG. 7. **The effect on band 3 transport sites of extensive papain cleavage of the transport domain.** Shown is the $^{35}Cl^-$ linebroadening due to band 3 transport sites on ghost membranes (*stripped ghosts*) and papain-treated ghost membranes (*stripped papain-treated ghosts*). Both types of membranes were stripped with high pH at low ionic strength, then washed in high salt and sonicated. Samples and ^{35}Cl NMR spectra were as in Fig. 3. The nonlinear least-squares best-fit curves ($y = Ax/(1 + xK_D)$, *solid lines*) yielded $K_D = 70 \pm 10$ mM and $K_D = 270 \pm 90$ mM for chloride binding to transport sites on stripped ghosts and stripped papain-treated ghosts, respectively.

The Effect of Extensive Papain Digestion on the Transport Site—It has just been shown that extensive papain digestion reduces all of the integral ghost proteins, including band 3, to small fragments protected by the membrane. In general, extensive proteolysis destroys band 3 catalyzed anion transport, as has been demonstrated for chymotrypsin (46), Pronase (37), and to a lesser degree of inhibition, extracellular papain (41). A likely cause of such transport inhibition is blockage of bound chloride translocation across the membrane, since this translocation involves a conformational change that could require structural integrity throughout large regions of the transport domain. In contrast, the transport site itself could be localized within a small region that is stearically protected, so that extensive digestion with a protease such as papain could leave the site relatively intact.

The effect of extensive papain digestion of the $^{35}Cl^-$ linebroadening due to the transport site is shown in Fig. 7, where the transport site linebroadening is identified by its sensitivity to DNDS (4). Transport site linebroadening *versus* $[Cl^-]^{-1}$ data are shown for two types of sonicated ghost membranes: 1) stripped ghosts and 2) stripped papain-treated ghosts. The stripped papain-treated ghosts correspond to SDS-PAGE, *lanes c–e* in Fig. 5. The papain treatment reduces the transport site linebroadening to <20% of its control value. Also, the linebroadening due to papain-treated transport sites approaches zero slope at lower $[Cl^-]^{-1}$ than does the control linebroadening, indicating that the papain treatment reduces the affinity of the transport site for chloride (Equation 2, see below). Thus, the papain digestion significantly alters the structure of the transport site; however, a DNDS-sensitive site that could be a damaged transport site does remain after proteolysis.

Verification of the Identity of the Transport Site Following Extensive Papain Digestion—The DNDS-sensitive site produced by extensive papain digestion cannot be *a priori* identified as the transport site because the affinities of the two sites for chloride are significantly different. Thus, the relationship between the two sites must be further examined; here the effect of transport site inhibition on the papain-generated site is studied.

H_2DIDS is a highly specific covalent inhibitor of the band 3 transport site. Under appropriate labeling conditions, one molecule of H_2DIDS can be incorporated per band 3 monomer, with negligible labeling of other ghost proteins (2). The effect of H_2DIDS transport site inhibition on the $^{35}Cl^-$ linebroadening due to the papain-generated site is shown in Fig. 8. Total linebroadening *versus* $[Cl^-]^{-1}$ data are shown for ghost membranes made from red cells labeled or unlabeled with H_2DIDS, then digested with papain and stripped. The linebroadening due to the papain-generated site is inhibited by H_2DIDS, although some positive slope is observed because the H_2DIDS labeling was only 62% complete (as determined from residual transport site linebroadening of unproteolyzed ghosts). The linebroadenings due to both the unlabeled and labeled membranes are further inhibited, to the same final extent, by 1 mM DNDS (Fig. 8). The results indicate that the papain-generated site is, in fact, the H_2DIDS-sensitive transport site, and that DNDS inhibits both the transport site linebroadening and some linebroadening due to low-affinity ($K_D \gg 400$ mM) chloride binding sites as well.

Phenylglyoxal is an arginine-specific covalent inhibitor of the band 3 transport site that, like H_2DIDS, can be used to test the identity of the papain-generated site. Phenylglyoxal labels band 3 at several sites in addition to the transport site (25, 47); however, the transport site is protected against phenylglyoxal labeling by the presence of DNDS (18, 25). The effect of phenylglyoxal inhibition of the transport site on the $^{35}Cl^-$ linebroadening due to the papain-generated site is shown in Fig. 9. Total linebroadening *versus* $[Cl^-]^{-1}$ data are shown for ghost membranes labeled with phenylglyoxal in the presence or absence of DNDS protection, then digested with papain and stripped. The linebroadening due to the papain-generated site is inhibited by phenylglyoxal, and DNDS protects the site against this phenylglyoxal inhibition. The linebroadenings due to both the protected and unprotected membranes are further inhibited to the same final extent by 1 mM DNDS (Fig. 9). These results are completely consistent with

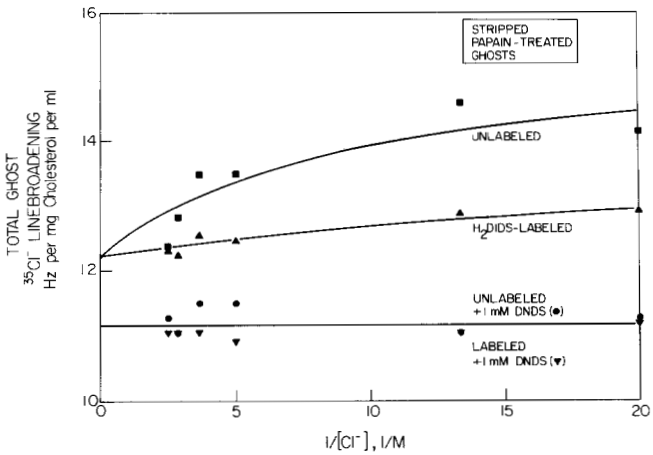

FIG. 8. **The effect of H_2DIDS on the papain-modified band 3 transport site.** Shown is the $^{35}Cl^-$ linebroadening from transport sites and low-affinity chloride binding sites on stripped papain-treated ghosts. Red cells were labeled or unlabeled with H_2DIDS; then leaky ghost membranes were prepared and the ghosts were proteolyzed with papain, stripped with high pH at low ionic strength, washed in high salt, and sonicated. Final samples were with or without 1 mM DNDS. Samples and ^{35}Cl NMR spectra were as in Fig. 3. The nonlinear least-squares best-fit curve ($y = A + Bx/(1 + xK_D)$) yielded K_D = 110 ± 50 mM for chloride binding to the papain-modified transport sites on unlabeled membranes (*upper curve*). The same function was used to best-fit the data for membranes labeled with H_2DIDS (*middle curve*) since only 62% of the band 3 transport sites were actually inhibited by H_2DIDS (see text). Only low-affinity sites ($K_D \gg 400$ mM) remain on both labeled and unlabeled membranes in the presence of 1 mM DNDS (*lower line*); these data are fit by a straight line of zero slope.

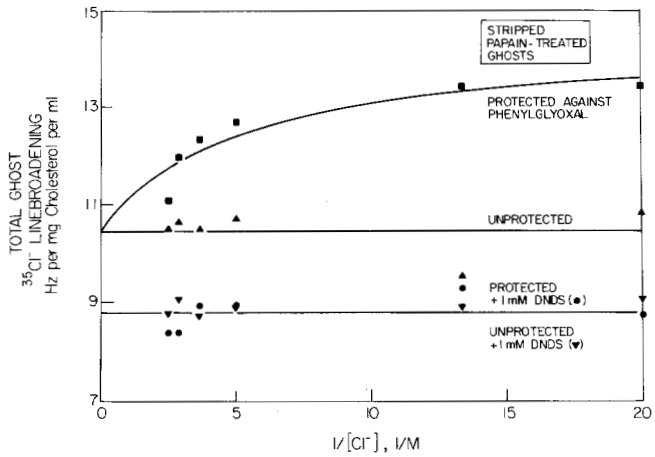

FIG. 9. **The effect of phenylglyoxal on the papain-modified band 3 transport site.** Shown is the $^{35}Cl^-$ linebroadening from transport sites and low-affinity chloride binding sites on stripped papain-treated ghosts. Red cells were labeled with phenylglyoxal in the presence or absence of DNDS to protect the transport site from labeling; then leaky ghost membranes were prepared and the ghosts were proteolyzed with papain, stripped with high pH at low ionic strength, washed in high salt, and sonicated. Final samples were with or without 1 mM DNDS. Samples and ^{35}Cl NMR spectra were as in Fig. 3. The nonlinear least-squares best-fit curve ($y = A + Bx/(1 + xK_D)$) yielded K_D = 200 ± 50 mM for chloride binding to the papain-modified transport site that had been protected by DNDS from phenylglyoxal (*protected, upper curve*). Only low-affinity sites ($K_D \gg$ 400 mM) remain when the transport site is not protected by DNDS from phenylglyoxal (*middle line*); these data are fit with a linear least-squares straight line of zero slope. Similarly, only low-affinity sites remain on the protected and unprotected membranes in the presence of 1 mM DNDS (*lower line*); these data are again fit by a linear least-squares straight line of zero slope.

TABLE I

Effect of nonintegral protein removal and protease treatment on low-affinity chloride binding sites

Treatment	Low-affinity site $^{35}Cl^-$ linebroadening[a]
	%
Control	100[b]
High-salt wash	104[b]
High pH, low ionic strength stripping followed by high-salt wash	85[b]
Trypsin in both compartments	68[c]
Chymotrypsin in both compartments	81[c]
Papain in both compartments	57[c,d]

[a] Data from the same experiments used to generate Figs. 3, 4, 6, and 9. The low-affinity site linebroadening is simply the DNDS-insensitive component of the linebroadening, except where indicated.
[b] Relative to unproteolyzed, unstripped sonicated ghost membranes.
[c] Relative to unproteolyzed, stripped sonicated ghost membranes.
[d] The low-affinity site linebroadening from papain-treated membranes is the phenylglyoxal-insensitive component of the linebroadening.

those already described for H_2DIDS; together, the phenylglyoxal and H_2DIDS experiments indicate that 1) the band 3 transport site is damaged, but not destroyed by the papain cleavage; 2) the chloride dissociation constant for this papain-modified site is 190 ± 80 mM (an average of the values derived from Figs. 7–9); 3) approximately ⅔ of the DNDS-sensitive linebroadening stems from the transport site; and 4) the remaining ⅓ of the DNDS-sensitive linebroadening stems from low-affinity chloride binding sites ($K_D \gg 400$ mM). Thus, DNDS, which specifically inhibits the transport site linebroadening in the ghost membrane system, is no longer specific for the transport site after the papain digestion. Instead, the papain digestion appears to create new DNDS binding sites such that DNDS inhibits some of the low-affinity chloride binding sites in addition to the papain-modified transport site. In contrast, H_2DIDS and phenylglyoxal, which are covalently attached before the papain digestion, specifically inhibit the papain-modified transport site.

The Effect of Nonintegral Protein Removal and Proteolysis on the Low-affinity Chloride Binding Sites—The total $^{35}Cl^-$ linebroadening due to leaky ghost membranes is composed of both transport site linebroadening and linebroadening due to low-affinity chloride binding sites ($K_D \gg 400$ mM (4)). The nonintegral ghost proteins contribute to the low-affinity site linebroadening, since stripping removes 15% of the low-affinity site linebroadening (Table I). The integral proteins also contribute, since trypsin, chymotrypsin, and papain remove an additional 17, 4, and 28% of the low-affinity site linebroadening, respectively (Table I). The identity and function of the low-affinity sites are unknown; however, since band 3 is the major polypeptide in ghost membranes, some or all of the low-affinity sites associated with integral proteins may be on band 3.

DISCUSSION

^{35}Cl NMR provides a powerful approach to the elucidation of the structure of the band 3 anion transport site. This technique enables study of two fundamental steps in the anion transport cycle: 1) migration of substrate chloride ion to the vicinity of the transport site, and 2) binding of chloride to the site. Since sealed vesicles are not needed for such studies, the ^{35}Cl NMR technique yields easily quantified information concerning the intactness of the transport site. Thus, the ^{35}Cl NMR technique can be used to determine the minimal struc-

ture containing the intact transport site, even if that minimal structure can no longer transport anions.

The results presented here indicate that the minimal structure containing the intact transport site includes neither the red cell nonintegral membrane proteins nor the band 3 cytoskeletal domain, since removal of these components from the transport domain leaves the transport site intact. Thus, no significant interaction occurs between the transport site and the cytoskeletal domain with its associated nonintegral proteins.

The transport site also remains intact when the transport domain is cleaved by chymotrypsin into 17- and 35-kDa fragments, even though both fragments contain residues known to lie in the vicinity of the transport site (see Introduction). Thus, strong attractive forces must hold these fragments together after proteolysis; direct evidence for these attractive forces has been obtained in H_2DIDS cross-linking studies (19). These results remain completely consistent with the possibility that the transport site may be composed of residues from more than one region of the primary structure.

Data presented here also indicate that extensive proteolysis on both sides of the membrane by papain cleaves the integral red cell membrane proteins into a mixture composed primarily of small papain fragments in the range 3–7 kDa, where the most prominant size is approximately 5 kDa. These data suggest that extensive papain cleavage followed by stripping removes approximately 60% or more of that portion of the transport domain protruding from the membrane into the solution (assuming 7 α-helical transmembrane segments/52-kDa transport domain (13), 3 kDa/40-Å α-helical transmembrane segment, and 5 kDa/average transmembrane segment produced by papain cleavage). Removal of the majority of the extramembrane material from the transport domain damages, but does not destroy, the transport site: thus, the transport site is composed of residues from one or more of the papain-generated fragments. These results are completely consistent with a picture in which 1) the transport site is buried near the center of the membrane, 2) the transmembrane segments that surround the transport site are held together by strong attractive forces within the membrane itself, and 3) an anion channel leads from the transport site to the solution so that anions can visit the buried transport site. Such a picture explains both the protection of the transport site from proteolysis and the existence of channel-blocking inhibitors that interfere with exchange of chloride between the transport site and solution (18). The picture also explains the fluorescence energy transfer data of Rao *et al.* (48), which show that the stilbenedisulfonate binding site is 34–42 Å from cysteine residues on the cytoskeletal domain. This distance is less than the thickness of the bilayer; thus, the stilbenedisulfonate binding site, including the transport site, is in the interior of the membrane. The picture appears physically reasonable: 1) the hydrophobic environment of the membrane interior would enhance the affinity of the transport site positive charge(s) for substrate anion; 2) the observation that the transmembrane translocation of bound chloride is the rate-limiting step in the transport cycle (33) is not inconsistent with the presence of anion channels leading to the transport site since anion migration through a transmembrane channel such as gramicidin is two orders of magnitude faster than the turnover rate of band 3 (2); 3) the reduction in the width of the anion permeability barrier due to anion channels leading to the transport site would not place an unreasonably larger electric field across the region of the transport domain between channels, assuming that fixed charges on the transport domain exist to counteract the transmembrane electric field in the vicinity of the transport site; and 4) the presence of channels leading to the transport site simplifies the transport process by shortening the distance over which the anion-transport site complex must be translocated.

The observation that proteolytic cleavage of the transport domain into transmembrane fragments does not destroy the transport site will greatly facilitate future structural studies of band 3, and a similar approach may be useful in a variety of systems involving transmembrane proteins (14). In the band 3 system, the ability to isolate the transmembrane segment(s) that are components of the transport site will greatly simplify both the identification of the essential residues in the transport site and the analysis of the associations between transmembrane segments that give rise to transport site structure.

REFERENCES

1. Macara, I. G., and Cantley, L. C. (1983) *Cell Membr.* **1,** 41–87
2. Knauf, P. A. (1979) *Curr. Top. Memb. Transp.* **12,** 249–363
3. Bennett, V. (1982) *Biochim. Biophys. Acta* **689,** 475–484
4. Falke, J. J., Pace, R. J., and Chan, S. I. (1984) *J. Biol. Chem.* **259,** 6472–6480
5. Bennett, V., and Stenbuck, P. J. (1979) *Nature* **280,** 468–473
6. Hargreaves, W. R., Giedd, K. N., Verkleij, A., and Branton, D. (1980) *J. Biol. Chem.* **255,** 11965–11972
7. Grinstein, S., Ship, S., and Rothstein, A. (1978) *Biochim. Biophys. Acta* **507,** 294–304
8. Bennett, V., and Stenbuck, P. J. (1980) *J. Biol. Chem.* **255,** 6424–6432
9. Steck, T. L., Ramos, B., and Stapazor, E. (1976) *Biochemistry* **15,** 1154–1161
10. Jenkins, R. E., and Tanner, M. J. A. (1977) *Biochem. J.* **161,** 139–147
11. Drickamer, L. K. (1976) *J. Biol. Chem.* **251,** 5115–5123
12. Cabantchik, Z. I., and Rothstein, A. (1974) *J. Membr. Biol.* **15,** 227–248
13. Jennings, M. L., Adams Lackey, M., and Denney, G. H. (1984) *J. Biol. Chem.* **259,** 4652–4660
14. Ramjessingh, M., Gaarn, A., and Rothstein, A. (1984) *Biochim. Biophys. Acta* **769,** 381–389
15. Falke, J. J., Pace, R. J., and Chan, S. I. (1984) *J. Biol. Chem.* **259,** 6481–6491
16. Wieth, J. O., Bjerrum, P. J., and Borders, C. L. (1982) *J. Gen. Physiol.* **79,** 293–312
17. Zaki, L. (1982) in *Protides of the Biological Fluids* (Peters, H., ed) pp. 279–328, Pergamon Press, New York
18. Falke, J. J., and Chan, S. I. (1984) *Biophys. J.* **45,** 91–92
19. Jennings, M. L., and Passow, H. (1979) *Biochim. Biophys. Acta* **554,** 498–519
20. Shami, Y., Rothstein, A., and Knauf, P. A. (1978) *Biochim. Biophys. Acta* **508,** 357–363
21. Ramjeesingh, M., Gaarn, A., and Rothstein, A. (1979) *Biochim. Biophys. Acta* **599,** 127–139
22. Drickamer, L. K. (1977) *J. Biol. Chem.* **252,** 6909–6917
23. Mayby, W. J., and Findlay, J. B. C. (1982) *Biochem. J.* **205,** 465–475
24. Rudloff, V., Lepke, S., and Passow, H. (1983) *FEBS Lett.* **163,** 14–21
25. Bjerrum, P. J., Wieth, J. O., and Borders, C. L. (1983) *J. Gen. Physiol.* **81,** 453–484
26. Nanri, H., Hamasaki, N., and Minakami, S. (1983) *J. Biol. Chem.* **258,** 5985–5989
27. Stadtman, T. C. (1957) *Methods Enzymol.* **3,** 392–394
28. Laemmli, U. K. (1970) *Nature* **227,** 680–685
29. Downer, N. W., Robinson, N. C., and Capaldi, R. A. (1976) *Biochemistry* **15,** 2930–2936
30. Merle, P., and Kadenbach, B. (1980) *Eur. J. Biochem.* **105,** 499–507
31. Oakley, B. R., Kirsch, D. R., and Morris, R. (1980) *Anal. Biochem.* **105,** 361–363
32. Forsén, S., and Lindman, B. (1981) *Methods Biochem. Anal.* **27,** 289–486
33. Falke, J. J., and Chan, S. I. (1985) *J. Biol. Chem.* **260,** 9537–9544

34. Heast, C. W. M. (1982) *Biochim. Biophys. Acta* **694,** 331–352
35. Steck, T. L. (1974) *Meth. Membr. Biol.* **2,** 245–381
36. Fukuda, M., Dell, A., Oates, J. E., and Fukuda, M. N. (1984) *J. Biol. Chem.* **259,** 8260–8723
37. Passow, H., Fasold, H., Lepke, S., Pring, M., and Schukman, B. (1977) in *Membrane Toxicity* (Miller, M. W., and Shamoo, A. E., eds) pp. 353–377, Plenum, New York
38. Markowitz, S., and Marchesi, V. T. (1981) *J. Biol. Chem.* **256,** 6463–6468
39. Tsuji, T., Irimura, T., and Osawa, T. (1981) *Carbohydr. Res.* **92,** 328–332
40. Matsuyama, H., Kawano, Y., and Hamasaki, N. (1983) *J. Biol. Chem.* **258,** 15376–15381
41. Jennings, M. L., and Adams, M. F. (1981) *Biochemistry* **20,** 7118–7123
42. Arnon, R. (1970) *Methods Enzymol.* **19,** 226–244
43. Marchesi, V. T., Furthmayr, H., and Tomita, M. (1976) *Annu. Rev. Biochem.* **45,** 667–698
44. Jones, M. N., and Nickson, J. K. (1981) *Biochim. Biophys. Acta* **650,** 1–20
45. Drickamer, L. K. (1978) *J. Biol. Chem.* **253,** 7242–7248
46. DuPre, A., and Rothstein A. (1981) *Biochim. Biophys. Acta* **646,** 471–478
47. Zaki, L. (1984) *FEBS Lett.* **169,** 234–240
48. Rao, A., Martin, P., Reithmeier, R. A. F., and Cantley, L. C. (1979) *Biochemistry* **18,** 4505–4516